View metadata, citation and similar papers at core.ac.uk

brought to you by CORE

provided by CURVE/open

The Ci(SiI)n defect in neutron-irradiated silicon

Londos, C. A., Christopoulos, S., Chroneos, A., Angeletos, T., Potsidi, M. & Antonaras, G.

Author post-print (accepted) deposited by Coventry University's Repository

Londos, CA, Christopoulos, S, Chroneos, A, Angeletos, T, Potsidi, M & Antonaras, G 2020, 'The Ci(SiI)n defect in neutron-irradiated silicon', Journal of Materials Science: Materials in Electronics, vol. 31, no. 2, pp. 930-934.
https://doi.org/10.1007/s10854-019-02602-4

Original citation & hyperlink:

DOI 10.1007/s10854-019-02602-4
ISSN 0957-4522
ESSN 1573-482X

Publisher: Springer

The final publication is available at Springer via http://dx.doi.org/10.1007/s10854-019-02602-4

Copyright © and Moral Rights are retained by the author(s) and/ or other copyright owners. A copy can be downloaded for personal non-commercial research or study, without prior permission or charge. This item cannot be reproduced or quoted extensively from without first obtaining permission in writing from the copyright holder(s). The content must not be changed in any way or sold commercially in any format or medium without the formal permission of the copyright holders.

This document is the author's post-print version, incorporating any revisions agreed during the peer-review process. Some differences between the published version and this version may remain and you are advised to consult the published version if you wish to cite from it.

The $C_i(Si_I)_n$ defect in neutron irradiated silicon

C. A. Londos[1,a)], S. -R. G. Christopoulos[2], A. Chroneos[2,b)], T. Angeletos[1], M. Potsidi[1], G. Antonaras[1],

[1]University of Athens, Solid State Physics section, Panepistimiopolis Zografos, Athens 157 84, Greece

[2]Faculty of Engineering, Environment and Computing, Coventry University, Priory Street, Coventry CV1 5FB, United Kingdom

Abstract

We report experimental results in neutron irradiated silicon containing carbon. Initially, carbon interstitial (C_i) defects form that readily associate with self-interstitials in the course of irradiation leading to the production of $C_i(Si_I)$ defects and upon annealing to the sequential formation of $C_i(Si_I)_n$ complexes. Infrared spectroscopy (IR) measurements report the detection of two localized vibrational bands at 953 and 960 cm^{-1} related with the $C_i(Si_I)$ defect. The thermal stability and annealing kinetics of the defect is discussed. The decay out of the two bands occurs in the temperature range of 130-200°C. They follow 2nd order kinetics with an activation energy of 0.93eV. No other bands were detected to grow in the spectra upon their annealing. Density functional the ory calculations were used to investigate the structure and the energetics of the $C_i(Si_I)$ and the $C_i(Si_I)_2$ defects.

Key words: Silicon; irradiation; IR spectroscopy; DFT calculations

Corresponding authors: a) C.A. Londos (hlontos@phys.uoa.gr) b) ab8104@coventry.ac.uk

1. INTRODUCTION

Silicon is an important material for the electronic industry used in numerous devices and applications (for example photovoltaics, sensors, nuclear medicine, integrated circuits, and quantum computing technologies).[1-5] A key element for the design and control of the performance of Si-based electronic devices is the impurities and defects present, which can affect the electrical, optical, mechanical and thermal properties. The defect reactions they participate in the various stages of material processing (for example irradiations, implantations, annealing) can play a key role for the quality of Si crystal.[6-11]

Carbon is an isovalent impurity that mainly occupies substitutional sites in the lattice (C_s). It is established that carbon reacts readily with self-interstitials (Si_I) and upon irradiation it is ejected at interstitial sites converted to C_i, through the Watkins replacement mechanism. The C_i impurity is very mobile around room temperature and leads to the formation of C_iC_s and C_iO_i defects [10, 12-15] which are very important defects in Si. Experimental results verify that the C_i, C_iC_s and C_iO_i defects are very effective traps for Si_I acting in essence as nucleation sites for them leading for the formation of larger complexes [16-19] such as $C_i(Si_I)_n$, $C_iC_s(Si_I)_n$ and $C_iO_i(Si_I)_n$, respectively.

Self-interstitials are very important impurities in Si affecting the physical properties and the behavior of the material. Notably, the formation of the $C_i(Si_I)_n$, $C_iC_s(Si_I)_n$ and $C_iO_i(Si_I)_n$ defects in Si wafer containing carbon acts competitively to the formation of large self-interstitial clusters which play a key role in several important processes in Si, as for instance transient enhanced diffusion (TED) of dopants and formation of extended defects.[20-23] Reaction processes involving the formation of the above three

families are always taken into account in data analysis and reaction modeling. Particularly, in radiation damage processes in Si such considerations are necessary to optimize the fabrication of the relative devices[17-19, 24]. In previous studies, we investigated the properties and behavior of $C_iO_i(Si_I)_n$ and the $C_iC_s(Si_I)_n$ complexes and mainly on the first two members (n=1,2) of the families.[10, 25-28]

Here we report IR studies on the $C_i(Si_I)_n$ family and mainly the $C_i(Si_I)$ and the $C_i(Si_I)_2$ defects. Two IR bands at 953 and 960 cm^{-1} have been previously correlated[29-31] with the $C_i(Si_I)$ complex although there is not any attribution of bands to the $C_i(Si_I)_2$ complex. We study the structure of the defects and the annealing kinetic of the $C_i(Si_I)$ complex. Density functional theory (DFT) calculations are used to gain insights on the structure and energetic of the $C_i(Si_I)$ and the $C_i(Si_I)_2$ defects.

2. METHODOLOGY

A. Experimental methodology

We used a group of mechanically polished Si samples with initial oxygen and carbon concentrations $[O_i]_o=7.2x10^{17}$ cm^{-3} and $[C_s]_o=1.53x10^{17}$ cm^{-3}. The used oxygen and carbon calibration coefficients were respectively 3.14 $x10^{17}$ cm^{-1} for the 1107 cm^{-1} oxygen band and 1.0 $x10^{17}$ cm^{-1} for the 605 cm^{-1}carbon band. The samples were irradiated with 5MeV fast neutrons at a fluence of ~ $1x10^{17}$ n/cm^2 at T~ 40 ^oC. They were wrapped in Cd foils to eliminate thermal neutrons and put inside sealed quartz boxes to avoid water contamination. After the irradiations, 20 min isochronal anneals of ~ 10^oC steps were performed in open furnaces. At the end of each annealing stage, infrared spectroscopy measurements were carried out, at room temperature, with a Jasco-IR 700 double beam

dispersive spectrometer with a spectral resolution of 1cm^{-1}. The background two-phonon absorption was always subtracted with the use of a reference sample of FZ silicon material.

B. Theoretical methodology

The DFT calculations were performed with the plane wave density functional theory code CASTEP.[32-36] Here the exchange-correlation interactions were considered with the corrected density functional of Perdew, Burke and Ernzerhof (PBE),[34] the generalized gradient approximation (GGA) was used with ultrasoft pseudopotentials.[31] The plane wave basis set cut-off was 350 eV, a 2 x 2 x 2 Monkhorst-Pack (MP)[32] k-point grid was used, in conjunction with a 250-atom supercell under constant pressure conditions. The convergence and efficacy of this theoretical methodology has been discussed in previous studies.[37-40]

3. RESULTS AND DISCUSSION

Fig. 1 presents the segments of the IR spectra in the range of 900 – 1040 cm^{-1} that are of interest. Three pairs of bands are shown: those of (934, 1018 cm^{-1}), (953,960 cm^{-1}) and (987,993 cm^{-1}) previously correlated with the $C_iO_i(Si_I)$, the $C_i(Si_I)$ and the $C_iC_s(Si_I)$ complexes, respectively.[29-31] In this investigation we shall focus on the $C_i(Si_I)$ complex detected experimentally after irradiation and formed as a result of the attachment of a self-interstitial atom to the C_i impurity in the course of irradiation.

Fig. 2 demonstrates the evolution with temperature of the 953 and 960 cm^{-1} bands of the $C_i(Si_I)$ defect. Notably, no other bands arise in the spectra upon annealing out of the above pair of bands.

The 953 and 960 cm^{-1} bands begin their annealing decay at the same temperature that is T_{anneal} ~135 ^{o}C and both anneal out at T~190 ^{o}C. In

order to calculate the activation energies of the two IR bans it would be necessary to study the annealing kinetics that governs the reactions which describe their decay. Using the methods of kinetic theory and the Arrhenius theory of the reactions, we can estimate the order of the kinetics as well as the activation energies of these two bands.

The general expression for the reaction kinetics that governs the annealing out of a defect is given[41] by the formula

$$-\frac{dN}{dt} = k_\gamma N^\gamma \quad (1)$$

where N is the defect concentration, γ is the order of the reaction and

$$k = k_0 e^{-\frac{E_a}{k_B T}} \quad (2)$$

is the rate constant of the reaction, where k_B is the Boltzmann constant. The parameters k_0 and E_a are the pre-exponential factor related to the so called attempt-to-escape frequency and the activation energy, respectively. They are both called Arrhenius parameters. The solution of the above differential equation depends on the value of γ. For the case of a first order kinetics reaction ($\gamma = 1$) we have the following expression[42-45]

$$N(\tau) = N(0)\, e^{-k_1 \tau} \quad (3)$$

while for the case of a second order kinetics reaction [42-45] ($\gamma = 2$) we have

$$N(\tau) = N(0)\, \frac{1}{1 + k_2 N(0) \tau} \quad (4)$$

where $N(0)$ and $N(\tau)$ are the initial concentration and the concentration after annealing time τ of the defect, respectively and k_1, k_2 the

corresponding rate constants as well. The diagram of $ln(k\tau)$ versus $1/T$ is the Arrhenius plot of the process. If the used value of γ produces a kinetics that best describes the experimental data, the Arrhenius plot is a straight line, from the slope of which we can estimate the average activation energy E_a of the process. Our results give a best fit[46] for $\gamma \sim 2$, corresponding to an absolute value of the correlation factor $|r| = 0.98$. For this case, the expression of $k_2\tau$ is

$$k_2\tau = \frac{1}{N} - \frac{1}{N(0)} \quad (5)$$

Fig.3 exhibits the Arrhenius plot for the decay of the 953 and 960 cm^{-1} bands, for the case of the second order kinetics. The activation energies for these bands are 0.93 and 0.92 eV, respectively.

The modeling[16] of the reaction process indicates the sequential formation of the $C_i(Si_I)_n$ family by the addition of self-interstitials. Thus the expected reaction that governs the annealing of our defect is

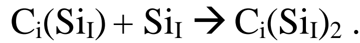

$C_i(Si_I) + Si_I \rightarrow C_i(Si_I)_2$.

We are compelled to accept that the concentrations of the $C_i(Si_I)$ and the Si_I are about the same to justify the second order kinetics. Sources of the self-interstitials are large defect clusters[47] produced in neutron irradiated Si. Reasonably, LVM modes related with the $C_i(Si_I)_2$ complex are expected to exist. However, no IR bands appear in our spectra concomittably with the decay of the $C_i(Si_I)$ complex bands. This is due to the fact that the related signals to the $C_i(Si_I)_2$ complex are very weak. Notably, the signals of the $C_i(Si_I)$ complex bands are just above the detection limit of our equipment. Moreover, the possibility of other reaction channels, as for instance $C_i(Si_I) + C_i(Si_I) \rightarrow (C_i)_2(Si_I)_2$, that lead to the parallel formation of other complexes as expected theoretically[19], is

an additional factor corroborating the absence experimentally of any bands of the $C_i(Si_I)_2$ complex.

DFT calculations can provide complementary information on the energetics and structure of the $C_i(Si_I)$ and the $C_i(Si_I)_2$ defects that is not easily accessible by experiment. To predict which the prevalent structure is we use energetic criteria and in particular binding energies. The binding energy to form a defect cluster is given by the energy difference between the defect cluster (i.e. energy of $C_i(Si_I)$) and the isolated constituent point defects (i.e. energy of C_i, Si_I). A negative binding energy translates to the defect cluster being more stable as compared to its constituent point defects.

Here we have employed DFT to investigate the stability of $C_i(Si_I)$ and the $C_i(Si_I)_2$ commencing with the C_i defect and gradually adding Si interstitials. The lowest energy structures for C_i, $C_i(Si_I)$ and $C_i(Si_I)_2$ are given in Figure 4. Considering first the $C_i(Si_I)$ defect the Si_I resides close to the C_i defect (distance 1.85 Å, refer to Fig. 4(b)). The binding energy of this defect is -1.93 eV suggesting that it is stable.

The addition of a further Si_I leads to the formation of the $C_i(Si_I)_2$ defect. Here we calculated that the most stable configuration of $C_i(Si_I)_2$ defect has a binding energy of -4.61 eV (refer to Fig. 4(c)), whereas a number of others are energetically close. The latter maybe an additional explanation, besides those mentioned above, on the reason why it is hard to detect a single IR peak for the $C_i(Si_I)_2$ defect – there could be more than one very weak peaks, related with various close configurations of the $C_i(Si_I)_2$ complex, that are hard to detect due to the low concentration of the defect.

4. CONCLUSIONS

We have investigated the $C_i(Si_I)_n$ family of defects, and especially the first two members (n=1,2), in neutron irradiated Si. We have verified the existence of two bands at 953 and 960 cm^{-1} previously correlated with the $C_i(Si_I)$ complex. We have studied the annealing kinetics of the center and we found that follows 2nd order kinetics with an activation energy of ~0.93 eV. The observed kinetics supports the reaction $C_i(Si_I) + Si_I \rightarrow C_i(Si_I)_2$. No band related with the $C_i(Si_I)_2$ complex was detected. DFT calculations were employed to investigate the structure and energetics of the $C_i(Si_I)$ and the $C_i(Si_I)_2$ defects. It is revealed that the $C_i(Si_I)_2$ defect is energetically bound to form with a binding energy of -4.61 eV, whereas other configurations were energetically close. This degeneracy in the energetics of the $C_i(Si_I)_2$ defect may explain the difficulty to identify a single IR signal experimentally. The present study aims to encourage further experimental investigations on this defect.

Acknowledgments

T. Angeletos is grateful to the A. S. Onassis Foundation for financial support though his Ph.D scholarship (grant No. G ZL 001-1/2015-2016).

References

1. W. W. Moses, Nucl. Instr. Meth. Phys. Res. A **610**, 11 (2009)
2. L. C. Andreani, A. Bozzola, P. Kowalczewski, M. Liscidini and L. Redorici, Adv. in Phys.: X, **4**, 1548305 (2018)
3. A. H. Atabaki, S. Moazeni, F. Pavanello, H. Gevorgyan, J. Notaros, L. Alloatti, M. T. Wade, C. Sun, S. A. Kruger, H. Meng, K. Al Qubaisi, I. Wang, B. Zhang, A. Khilo, C. V. Baiocco, M. A. Popović, V.M. Stojanović & R. J. Ram, NATURE **556**, 349 (2018)
4. G. Lindstrom, Nucl. Instr. Meth. Phys. Res. A **512**, 30 (2003)
5. H.-W. Hubers, S. G. Pavlov, V. N. Shastin, Semicond. Sci. Technol. **20**, S211(2005)
6. R. C. Newman, in Defects in Silicon II edited by W. M. Bullis, U. Gosele, F. Shimura, Proceedings Volume **91-9**, 271 (1991)
7. D. Tsuchiγa, K. Sueoka, and H. Yamamoto, Phys. Stat. Solidi A, 1800615, (2019) (DOI: 10.1002/pssa.201800615)
8. C. A. Londos, A. Andrianakis, E. N..Sgourou, V. V Emtsev and H. Oyama, J. Appl. Phys. **109 ,** 033508 (2011)
9. E. Simoen, S. K. Dhayalan, A. Hikavyy, R. Loo, E. Rosseel, H. Vrielinck, and J. Lauwaert, ECS J. Sol. Stat. Sci. Technol. **6**, P284 (2017)
10. H. Wang, A. Chroneos, E. N. Sgourou, C. A. Londos, and U. Schwingenschlogl, Sci. Rep. **4**, 4909 (2014)
11. A. Chroneos, E. N. Sgourou, C. A. Londos , and U. Schwingenschlogl, Appl. Phys. Rev. **2**, 021306 (2015)
12. C. A. Londos, phys. stat. sol. (a) **92**, 609 (1985)
13. C. A. Londos, Semicond. Sci. Technol. **5**, 645 (1990)
14. F. Zirkelbach, B. Stritzker, K. Nordlund, J. K. N. Lindner, W. G. Schmidt, and E. Rauls, Phys. Rev B **84,** 064126 (2011)

15. E. Simoen, S. K. Dhayalan, A. Hikavyy, R. Loo, E. Rosseel, H. Vrielinck, and J. Lauwaert, ECS J. Solid State Science and Technology **6**, P284 (2017)
16. G. Davies, Materials Science Forum, **38-41**, 151 (1989)
17. A. Matoni, F. Bernadini, and L. Colombo, Phys. Rev. B **66**, 195214 (2002)
18. B. C. MacEvoy, S. I. Watts, Solid State Phenomena **57-58**, 221 (1997)
19. R. Pinacho, P. Castrillo, M. Jaraiz, I. Martin-Bragado, J. Bartolla, H.-J. Gossmann, G.-H. Gilmer, and I.-L. Benton, J. Appl;. Phys. **92**, 1582 (2002)
20. A. E. Michael, W. Rausch, P. A. Ronsheim, R. H. Kastl, Appl. Phys. Lett. **50**, 416 (1987)
21. K. S. Jones, J. Liu, L. Zhang, V. Krishnamurtly, and R. T. DeHoff, Nucl. Instum. Methods Phys. Res. B **106,** 227 (1995)
22. S. Lee, and G. S. Hwang, Phys. Rev. B **78**, 045204 (2008)
23. S. S. Kapur, and T. Sinno, Phys. Rev. B **82**, 045205 (2010)
24. S. S. Kapur, M. Prasad, and T. Sinno, Phys. Rev. B **69**, 155214 (2004)
25. C. A. Londos, D. N. Aliprantis, G. Antonaras, M. S. Potsidi, and T. Angeletos, J. Appl. Phys. **123**, 145702 (2018)
26. S.-R.G. Christopoulos, E. N. Sgourou, R. V. Vovk, A. Chroneos, C. A. Londos, Solid State Commun. **263**, 19 (2017)
27. M. S. Potsidi and C. A. Londos, J. Appl. Phys. **100**, 033523 (2006)
28. S.-R.G. Christopoulos, E. N. Sgourou, R. V. Vovk, A. Chroneos, C. A. Londos, Materials, **11**, 612 (2018)
29. G. Davies and R.C. Newman, in Handbook of Semiconductors, edited by S. Mahajan (Elsevier, Amsterdam, 1994), Vol. **3**, p. 1557-1635

30. C. A. Londos, M. S. Potsidi and E. Stakakis, Physica B **340-342**, 551 (2003)
31. S. P. Chappell and R. C. Newman, Semicond. Sci. Technol. **2**, 691 (1987)
32. M. C. Payne, M. P. Teter, D. C. Allan, T. A. Arias, and J. D. Joannopoulos, Rev. Mod. Phys. **64**, 1045 (1992).
33. M. D. Segall, P. J. D. Lindan, M. J. Probert, C. J. Pickard, P. J. Hasnip, S. J. Clark, and M. C. Payne, J. Phys.: Condens. Matter **14**, 2717 (2002).
34. J. Perdew, K. Burke, and M. Ernzerhof, Phys. Rev. Lett. **77**, 3865 (1996).
35. D. Vanderbilt, Phys. Rev. B **41**, 7892 (1990).
36. H. J. Monkhorst and J. D. Pack, Phys. Rev. B **13**, 5188 (1976).
37. A. Chroneos, and C. A. Londos, J. Appl. Phys. **107**, 093518 (2010).
38. A. Chroneos, C.A. Londos, E. N. Sgourou, and P. Pochet, Appl. Phys. Lett. **99**, 241901 (2011).
39. E. N. Sgourou, D. Timerkaeva, C. A. Londos, D. Aliprantis, A. Chroneos, D. Caliste, and P. Pochet, J. Appl. Phys. **113**, 113506 (2013).
40. H. Wang, A. Chroneos, C. A. Londos, E. N. Sgourou, and U. Schwingenschlögl, Appl. Phys. Lett. **103**, 052101 (2013).
41. J. Bourgoin and M. Lannoo, *Point Defects in Semiconductors II Experimental Aspects* (Springer-Verlag, Berlin, Heidelberg/New York, 1983). ISBN-13:978-3-642-81834-9
42. S. Ishino, F. Nakazawa, and R. Hasiguti, J. Phys. Chem. Solids **24**, 1033 (1963)
43. P. W. Atkins, Physical Chemistry (Oxford University Press, 1994)
44. K. J. Laidler, Chemical Kinetics (Harper & Row, New York, 1987)

45.R. Radu, I. Pintilie, L. F. Makarenko, E. Fretwurst, and G. Lindstroem, Journal Appl. Phys. **123**, 161402 (2018)

46. Grow, F. Davis, and M. Maxfield, Statistical Manual, pp.157–158 (Dover, New York, 1960)

47. R. C. Newman, and R. Jones, in *Semiconductors and Semimetals,* edited by F. Shimura, Vol. **42**, 289 (Academic Press San Diego, 1994)

Figure Captions

Fig. 1 Fragment of the IR spectra of neutron irradiated silicon.

Fig. 2 The thermal evolution of the 953 and 960 cm^{-1} IR bands of the $C_i(Si_I)$ complex.

Fig. 3 Arrhenius plot for the decay of the 953 and 960 cm^{-1} IR bands.

Fig. 4 The lowest energy structures for (a) C_i, (b) $C_i(Si_I)$ and (c) $C_i(Si_I)_2$ as calculated by density functional theory.

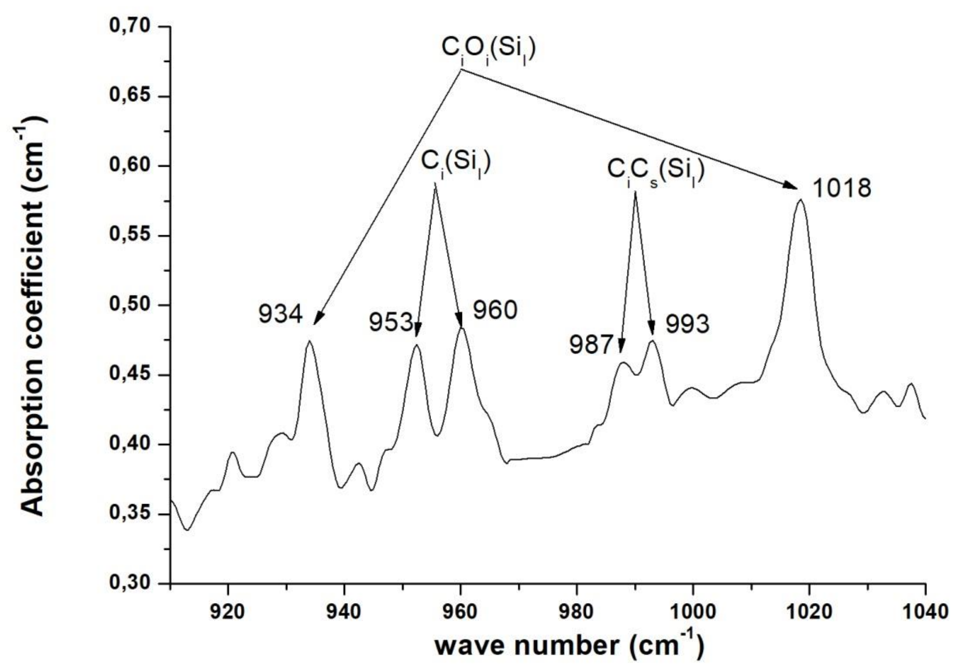

Fig.1

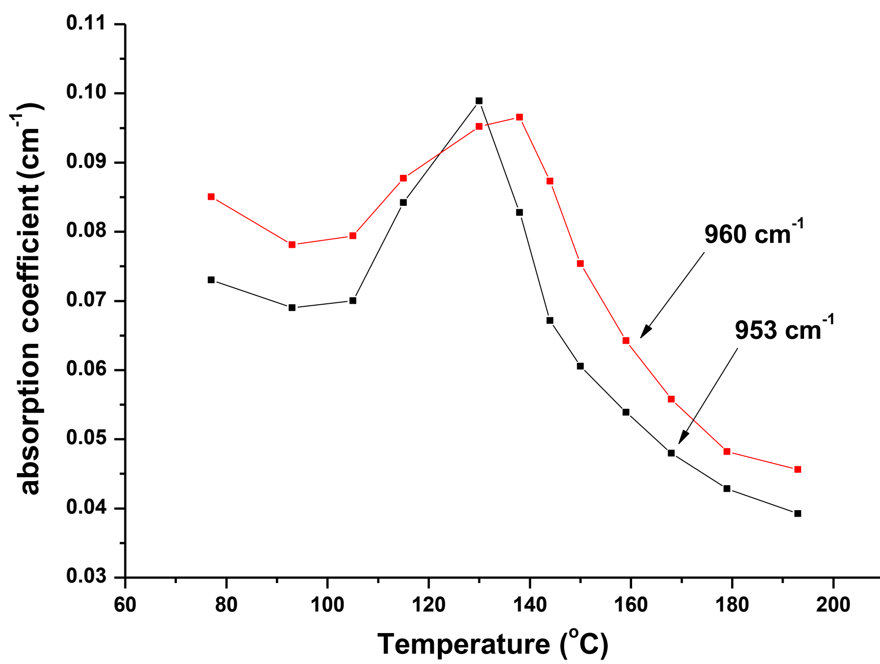

Fig.2

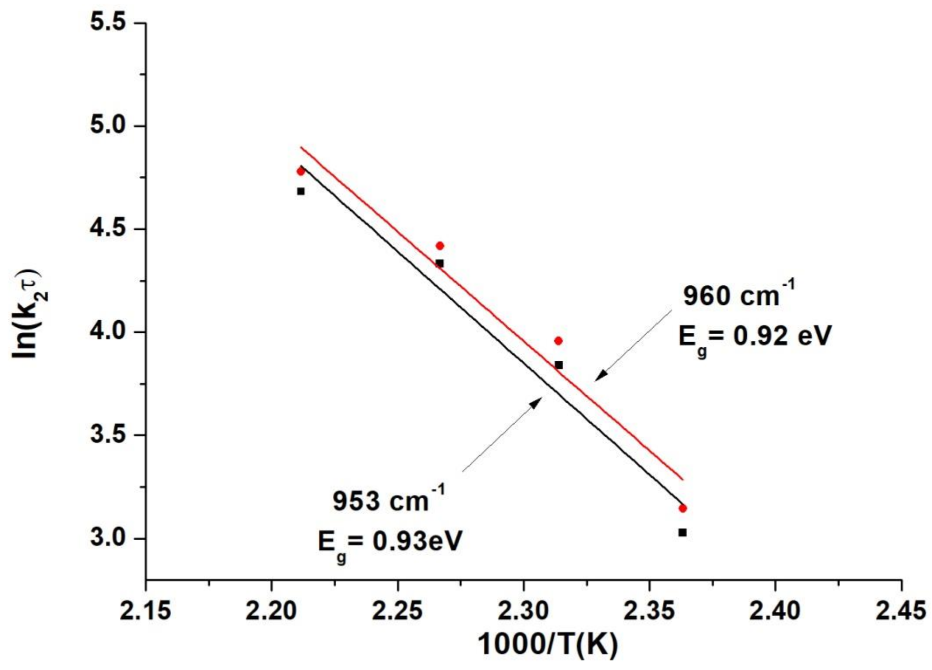

Fig.3

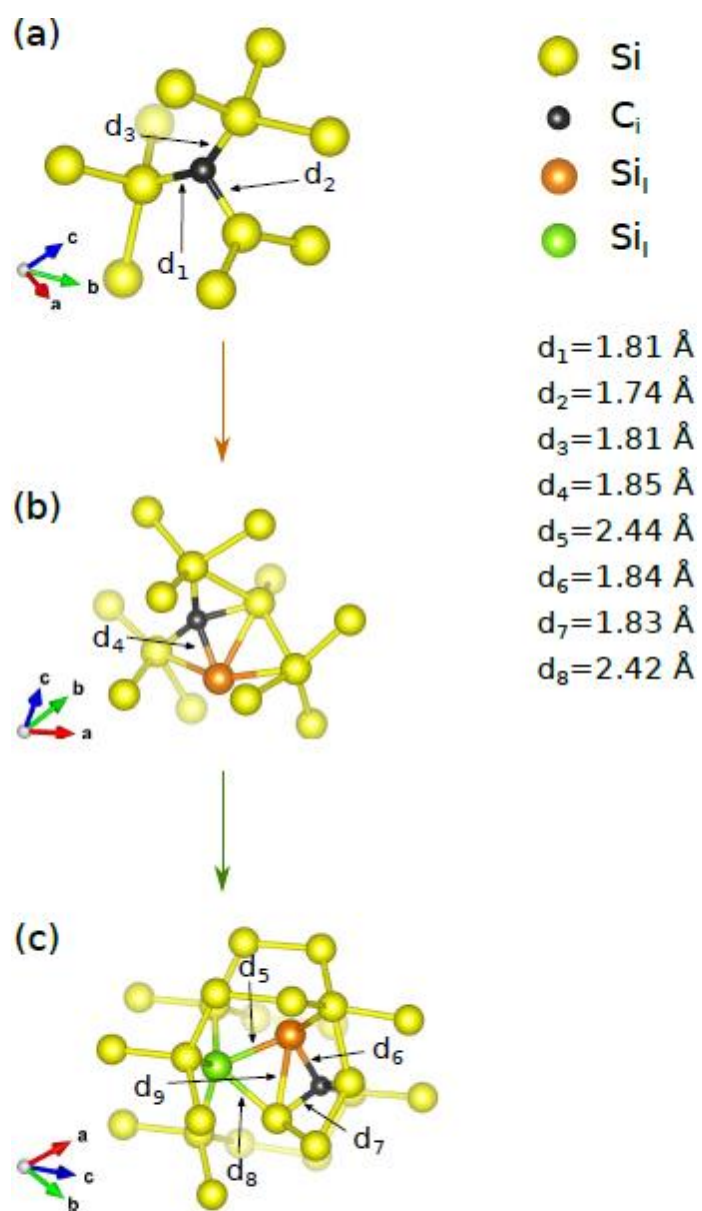

Fig. 4